Mechanical Properties of Sintered Iron-Boron Alloys

Pavan Suri, Randall M. German

Center for Innovative Sintered Products
P/M Lab
Pennsylvania State University
University Park, Pennsylvania 16802

Abstract:

The tensile strength and elongation of coarse iron and steel powder sintered with boron was investigated. The properties vary significantly with boron content due to decrease in porosity, precipitation of borides on the particle boundaries, and its contiguity. An increase in the contiguity of the ductile phase increases the tensile elongation. Results on the mechanical behavior of the sintered material, with a change in the contiguity of the ductile phase in the microstructure are presented.

Introduction:

Ferrous alloys sintered with the aid of boron exhibit increased tensile strength owing to an increase in density and the presence of hard, boride phase. However, at additive levels suitable to sinter coarse powders to near full density, there is often a reduction in the elongation attributed to the brittle, continuous boride phase along the particle boundaries. Such a reduction in ductility renders the material incapable of being used towards structural applications. Focus of the present study is directed towards the effect of boride phase and its continuity on the tensile properties of sintered ferrous alloys.

Unlike carbides [1], the morphology of the boride phase cannot be altered by thermo-mechanical treatment. Boron reacts with most of the transition metals to give stable borides [2]. The partially continuous, blocky precipitates that form along the particle boundaries, as shown in Figure 1, contributes to the embrittlement of the sintered alloy [3-10]. Addition of prealloyed powder was used as a processing strategy to avoid the formation of continuous precipitate boride along the particle boundaries. The effects of addition of prealloyed powder on density, microstructure and mechanical properties are examined.

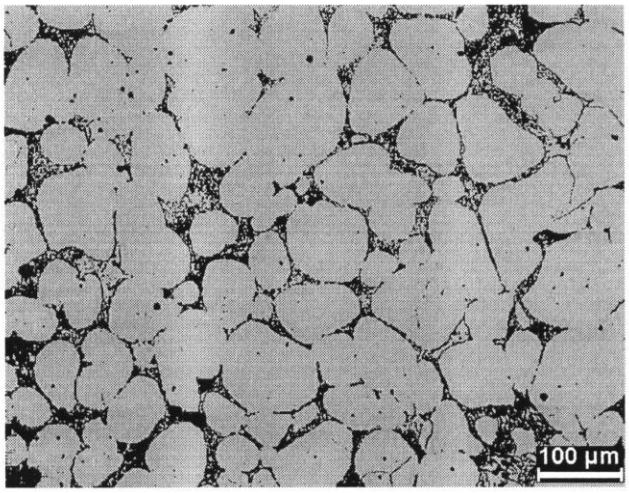

Figure 1: Micrograph of sintered ferrous compacts with boron additions, illustrating the partially continuous, blocky morphology of Fe_2B precipitated along the particle boundaries.

Materials and Experimental Procedures:

Tensile test specimens were prepared by sintering water atomized iron powder prealloyed with molybdenum and blended with various amounts of boron and water atomized, prealloyed 316L stainless steel powder. The characteristics and the composition of the powders used are given in Table 1 and Table 2 respectively. The morphology of the powders used in the study is given in Figure 2.

Table 1: Composition of the powders in weight percent.

	Fe	Mn	Mo	Cu	Ni	Cr	C	S	O	Si
A	Balance	0.13	1.44	0.06	0.05	0.04	<0.01	0.01	0.07	0.02
B	Balance	0.39	2.42	0.00	12.1	16.99	0.03	0.007	0.005	0.85

Table 2: Powder characteristics

	$\rho_{apparent}$, g/cm^3	ρ_{tap}, g/cm^3	$\rho_{pycnometer}$, g/cm^3	Flow rate, s/50g	D_{10}, µm	D_{50}, µm	D_{90}, µm
A	3.3	3.9	7.87	24.4	42	102	194
B	3.27	4.26	7.86	28.1	10	15	21

where, A denotes water atomized iron powder prealloyed with molybdenum and B denotes water atomized prealloyed 316L stainless steel powder.

The tensile bars of standard dog bone geometry were prepared using uniaxial pressing machine (Gasbarre Products Inc., Dubois, PA) at pressures of 600 MPa. The bars were sintered in a 6 zone CM pusher furnace (model: 330-30-IZ, supplier: CM Furnace, Bloomfield, NJ) at 1200°C for 30 minutes. Tensile testing was performed using an 88.9 N screw type tensile machine (model: Sintech 20/D, supplier: MTS Systems Corp, Eden Praire, MN) with a 20 kip load frame at a crosshead speed of 6.35 mm/min. Tensile elongation of the sample was measured by an extensometer (model: 634.12E-54, supplier: MTS Systems Corp, Eden Praire, MN). Microstructure of the samples, obtained via

standard polishing techniques, was etched with 2% nital and observed under an inverted stage microscope (model: Epiphot, supplier: Nikon, Tokyo, Japan).

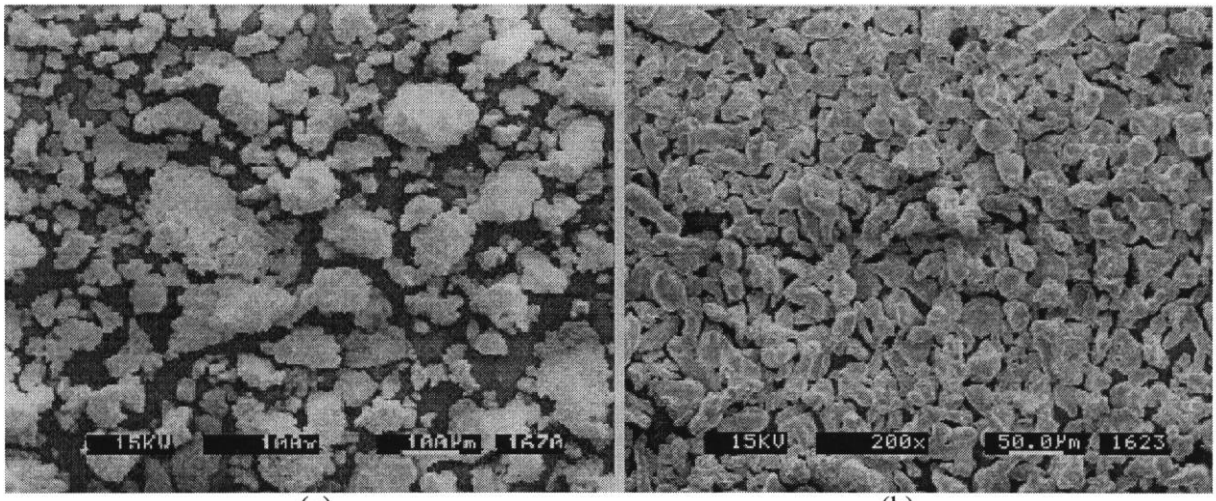

(a) (b)

Figure 2: Morphology of the (a) water atomized iron powder prealloyed with molybdenum and (b) water atomized, prealloyed 316L stainless steel powder used in the study.

Experimental Results and Discussion:

The addition of prealloyed powder increased the contiguity of the ductile phase and decreased the sintered density, as shown in Figure 2.

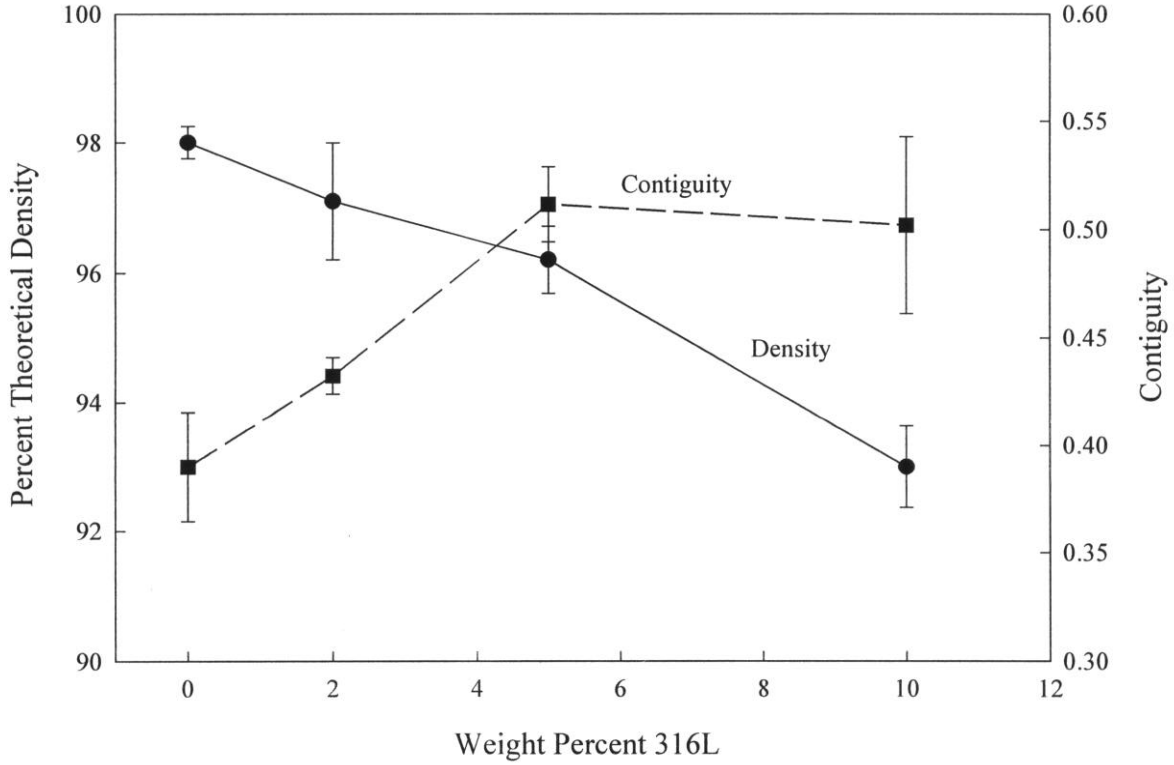

Figure 3: Variation in the contiguity of the ductile phase and the density of the sintered compact with addition of prealloyed 316L powder.

Changes in the microstructure associated with the addition of prealloyed 316L stainless steel powder is shown in Figure 3 (a)-(d). Decrease in the sintered density is due to the reduction in the amount of boron available to form a liquid phase at the sintering temperature. The microstructures, given in Figure 3 (a)-(d), reveal the rounded pores to be present near the prealloyed powder. Chromium forms CrB_2, a boride with a higher free energy of formation (more negative) than Fe_2B. CrB_2 nucleates within the prealloyed particle, as shown in Figure 4. The preferential precipitation of boride also contributes to an increase in the contiguity of the ductile phase.

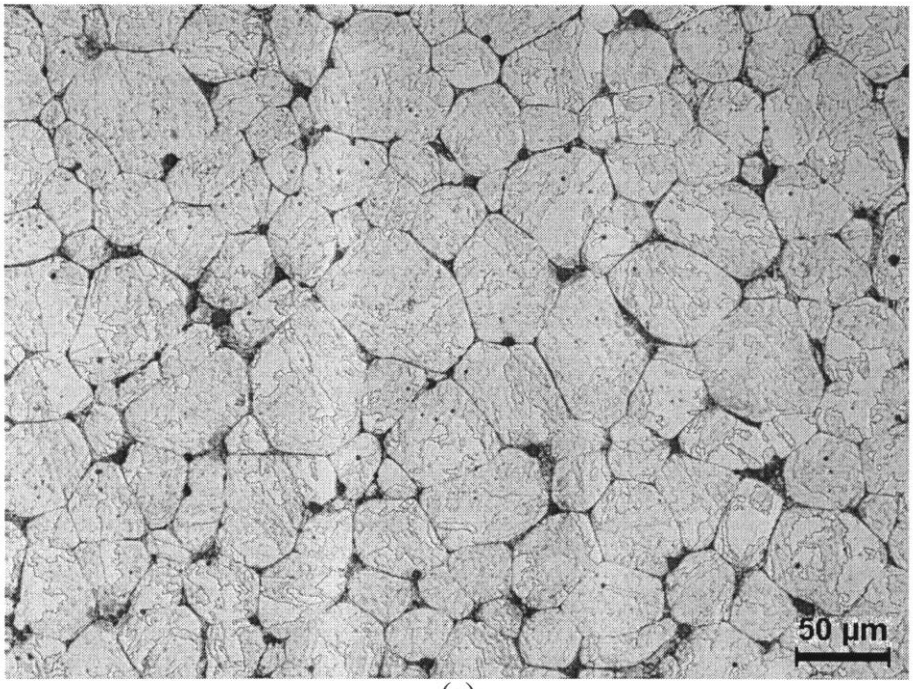

(a)

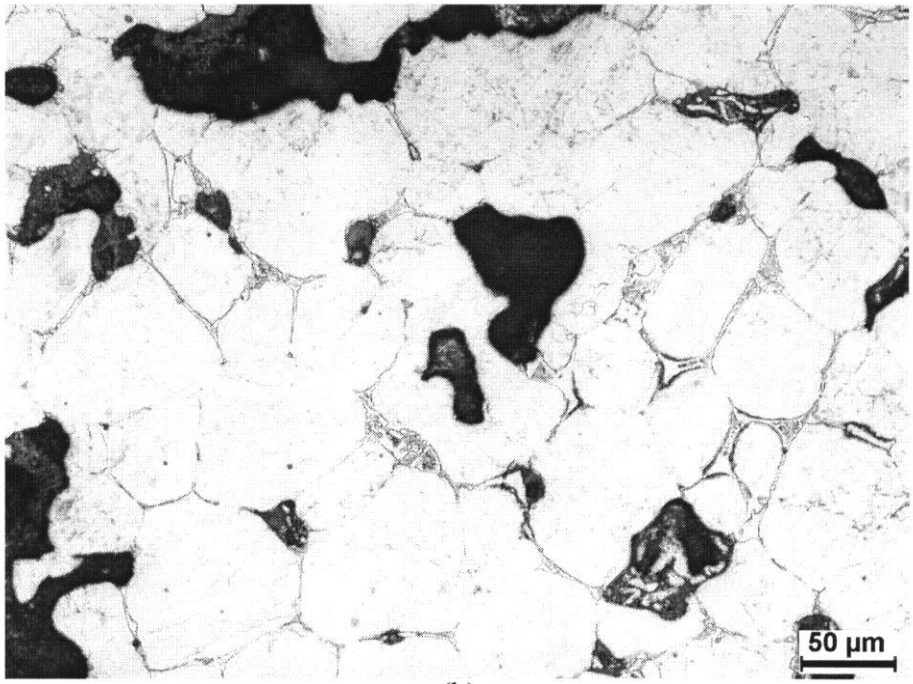

(b)

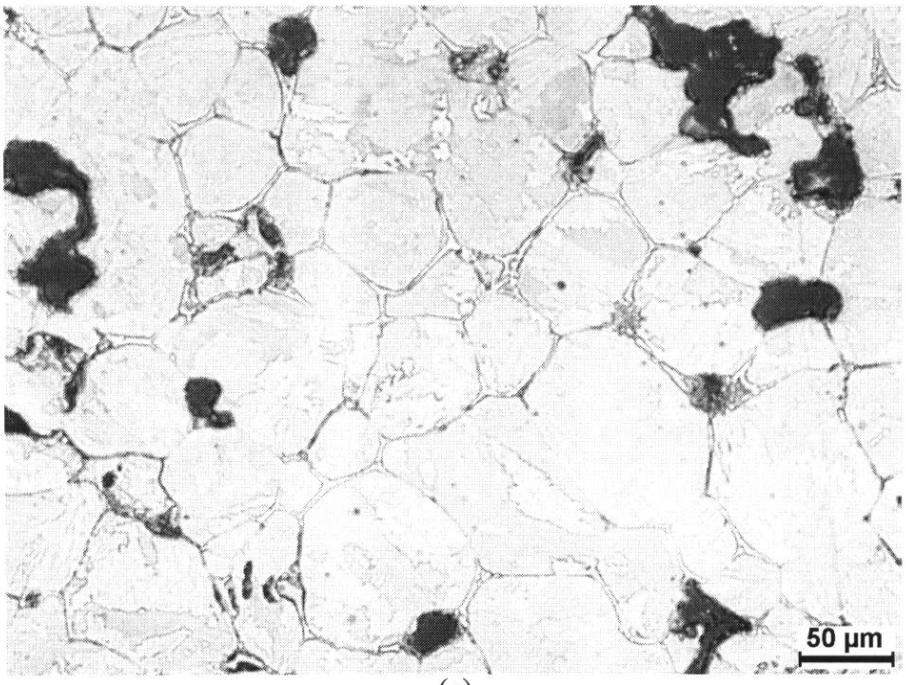

(c)

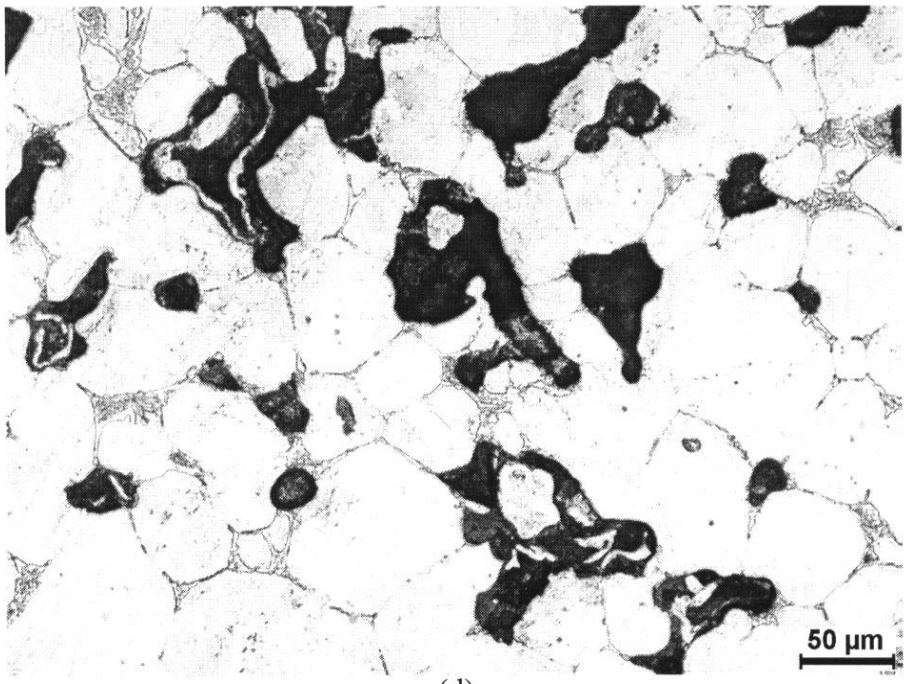

(d)

Figure 4: Micrographs of sintered Fe-1.5Mo powder with 0.4 weight percent boron additions admixed with (a) 0, (b) 2, (c) 5, and, (d) 10 weight percent prealloyed 316L. Micrographs reveal an increase in contiguity and a decrease in the sintered density with increasing prealloyed powder content.

The strength and ductility of the sintered alloy due to a change in the microstructure are given in Figure 5. The strength of the iron-boron alloys is not limited by the interfacial strength of the iron and iron boride. In such cases, failure in the coarse microstructure is initiated due to the microcracking of the hard phase [11].

Fracture of hard phase particles occurs due to the large shear stresses on the boride precipitates and inhomogeneity in plastic strain during uniaxial tensile deformation. This in turn contributes to a decrease in the plastic deformation. This is evident from the SEM micrographs of the fractured tensile specimens shown in Figure 6 (a) and (d). The sintered material without boron additions failed by ductile rupture. With an increase in the boron additions to 0.2 weight percent, the fracture surface exhibits a partially ductile and partial brittle, cleavage fracture.

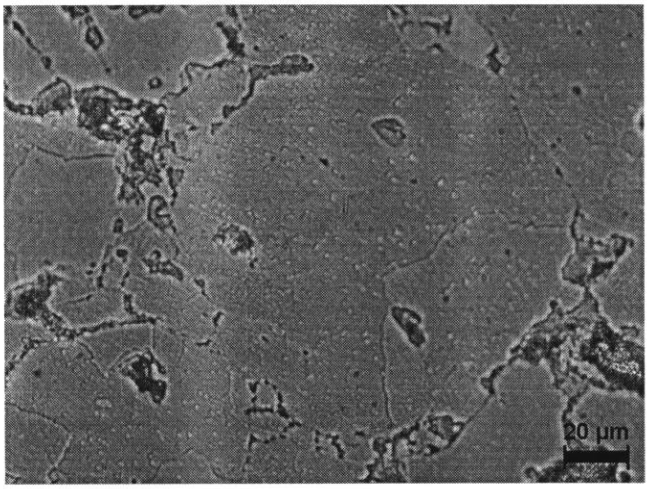

Figure 5: Micrograph showing the boride phase nucleated with in the prealloyed particle. The contrast was obtained by coating a layer of PtO_2 on the polished and etched surface.

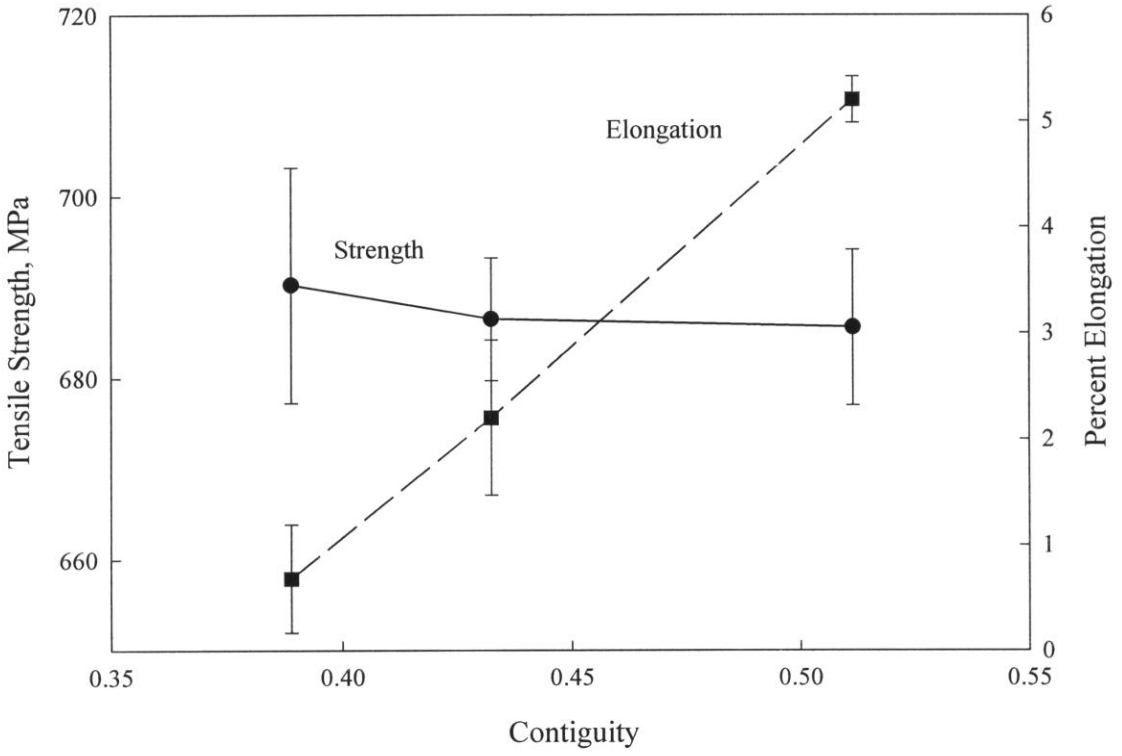

Figure 6: Tensile strength and elongation of sintered alloy with a change in contiguity of the ductile phase in the microstructure.

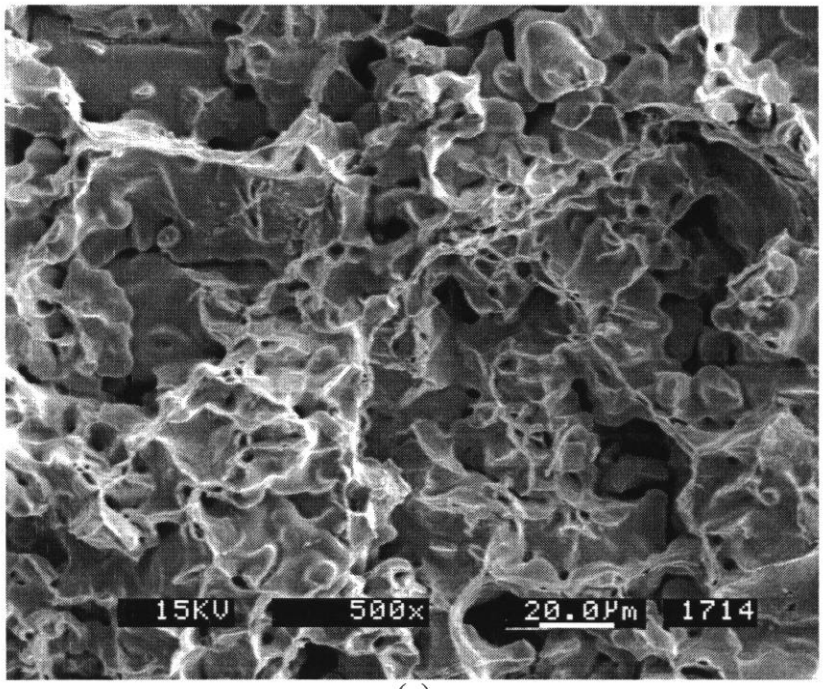

(a)

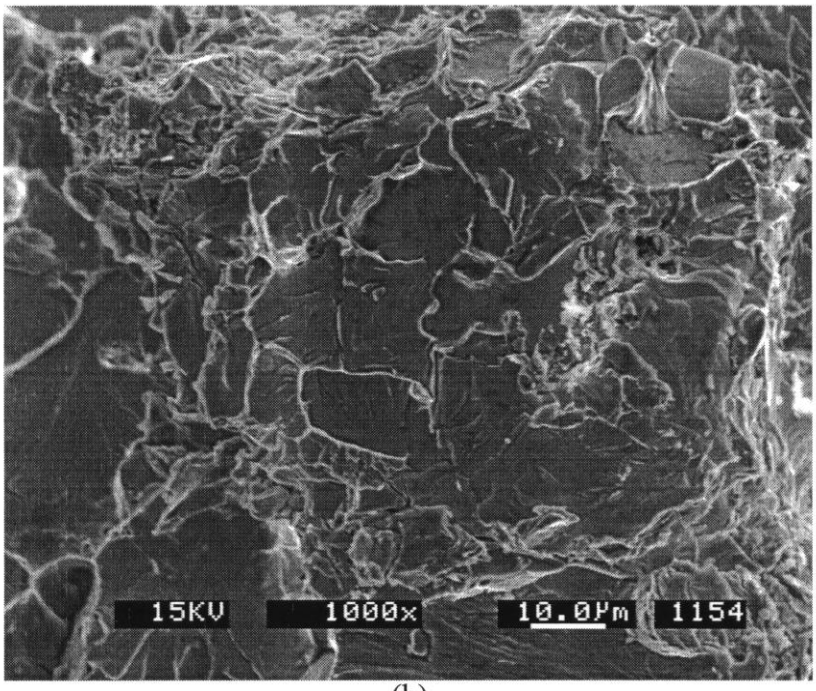

(b)

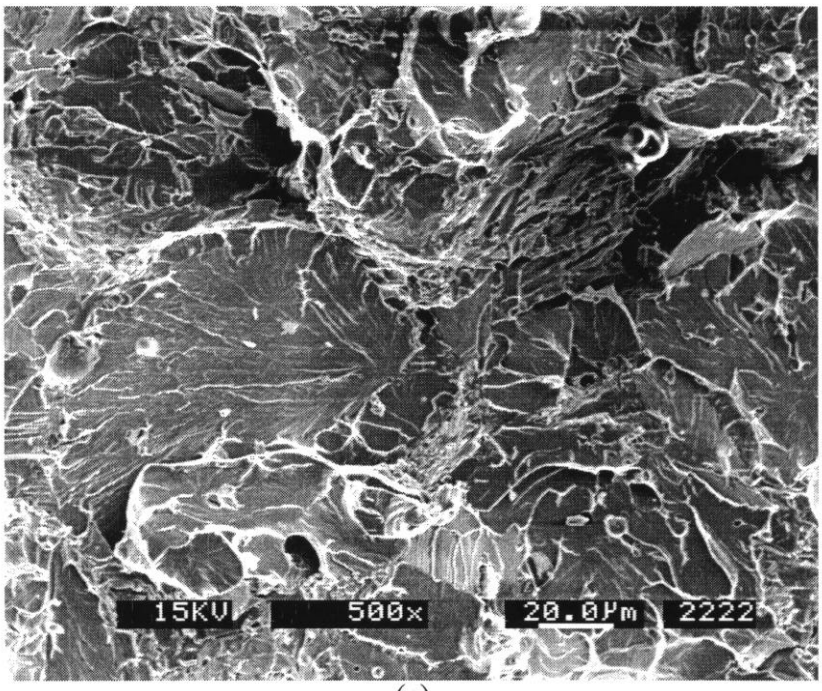

(c)

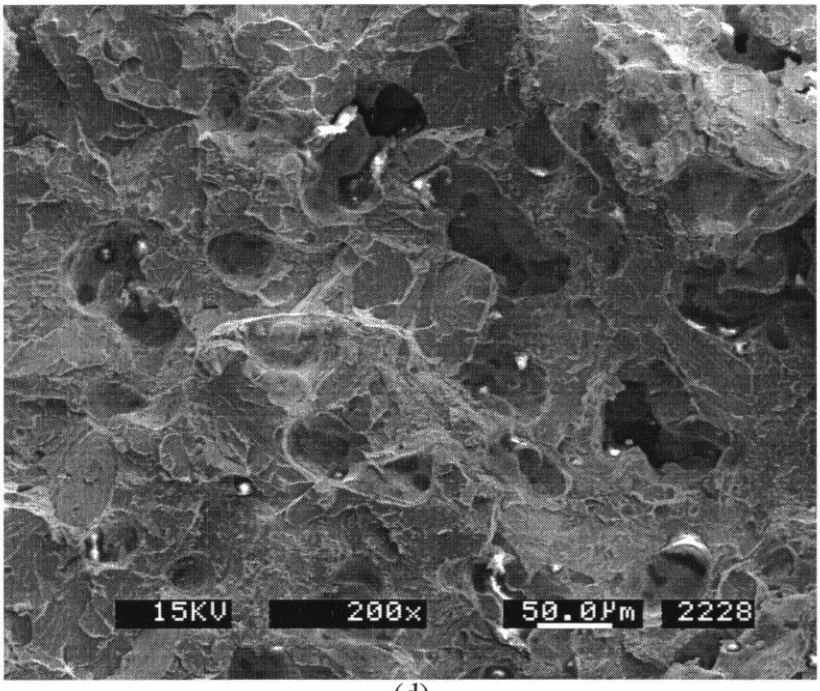

(d)

Figure 7: SEM micrograph of the fractured surface of tensile bars sintered with (a) 0, (b) 0.2, (c) 0.4 wt pct boron, and, (d) 0.4 wt pct boron with 5 wt pct prealloyed 316L powder.

The distance between the cleavage planes reveals the extent of plastic deformation. Plastic strain accommodation is also evident in Figure 7(b) in the form of microcracking. The stored elastic energy (in the matrix, due to strain incompatibility) is released in the form of microcracks. This is in contrast to flat fractured surface observed in Figure 7(c) indicating limited plastic deformation. The extent of brittleness due to the increased grain boundary coverage of the boride phase is evident from the spacing of the cleavage planes in Figure 7(c) in contrast to Figure 7(b). With an increase in the contiguity of the ductile phase (due the addition of prealloyed powder), the distance between the cleavage planes decreases as

evident from Figure 7(d). Hence, the tensile elongation increases with increase in the contiguity of the ductile phase. The increase in contiguity of the ductile phase also promotes plastic strain accommodation, observed in the case of compacts sintered with 0.2 weight percent boron additions.

It is important to establish in the present case that the increase in tensile elongation, as given in Figure 5, is due to the increase in the contiguity of the ductile phase and not a contribution of the austentic (316L) phase. The presence of austentic phase could increase the ductility as a result of crack-ductile phase (particle) interaction. Such an interaction manifests as crack bridging or crack deflection. The micrographs given in Figures 7(c) and (d) reveal that the presence of austenitic phase did not influence the fracture process or the failure path. This further reinforces the argument that the observed increase in the tensile elongation is due to change in contiguity.

Conclusion:

In a two-phase material, the harder phase is subjected to an excess stress [12]. During plastic deformation, the hard, second phase particles fracture and act as a sharp notch, leading to cleavage in ferrite. The plastic deformation in the ferrite phase depends on the extent to which it is constrained by the boride phase. Enhancing the contiguity of the ductile phase increases the tensile elongation and decreases the strength of the sintered alloy as expected. The extent and nature of boride phase precipitation has a significant impact on the optimization of the properties of sintered iron boron alloys.

Reference:

1. Uggowitzer P., Stuwe H.P., "The Tensile Fracture of Ferritic-Martensitic Carbon Steels", *Materials Science and Engineering*, Vol. 55, 1982, pp 181-189.
2. Shrivastava P.K., Tiwari A.N., Gopinathan V., "Role of Boron in Fe and Ni-Based Rapidly Solidified Microcrystallline Alloys", *Key Engineering Materials*, Vol. 38-39, 1989, pp. 143-162.
3. Tandon R., German R.M., "Sintering and Mechanical Properties of a Boron-Doped Austentic Stainless Steel", *International Journal of Powder Metallurgy*, Vol. 34, No. 1, 1998, pp. 40-49.
4. Madan D.S., German R.M., "Enhanced Sintering for Ferrous Components", *Modern Development in Powder Metallurgy*, Vol. 15, MPIF, APMI, 1984, pp. 441-454.
5. Molinari A.; Kazior J.; Marchetti F.; Canteri R.; Cristofolini I.; Tiziani A., "Sintering Mechanisms of Boron Alloyed AISI 316L Stainless Steel", *Powder Metallurgy*, Vol. 17,No.2, 1994, pp. 115-122.
6. Liu J.; Cardamone A.; Potter T.; German R.M., "Liquid Phase Sintering of an Iron-Carbon Alloy with Boron Additions", *Powder Metallurgy*, Vol. 43, No. 1, 2000, pp. 57-61.
7. Molinari A., Kazior J., Straffelini G., Pieczonka T., "Persistent Liquid Phase Sintering of 316L Stainless Steel", *International Journal of Powder Metallurgy*, Vol. 34, No. 2, 1998, pp. 21-28.
8. Selecka M., Danninger H., Salak A., Unami S., Parilak E., "Properties of Boron Liquid Phase Sintered of Cr-Mo-V Alloyed Steel", *Proceeding of the International Conference DF PM'99*, September 19-22, Vol. 1, 1999, Kosice, Slvoak Republic, pp. 175-182.
9. Selecka M., Salak A., Dudrova E., "Boron in Sintered Ferrous Alloys - Overview. Part I. Iron-Boron", *Powder Metallurgy Science and Technology*, Vol. 6., No. 2, 1995, pp. 1-12.
10. Myers N., Suri P., German R.M., "High Density P/M Steels", *Advances in Powder Metallurgy and Particulate Materials*, Vol. 6, 2000, pp. 63-68.
11. Tomota Y., Kawamura Y., "On Ductile Fracture of Steels Containing the Coarse Second Phase", *Bulletin of the JSME*, Vol. 24, No. 188, 1981, pp: 282-289.
12. Poech M.H., Fischmeister H.F., "Deformation of Two-Phase Materials: A Model Based on Strain Compatibility", *Acta Metallurgica et Materiala*, Vol. 40, No. 3, 1992, pp. 487-494.